

# Spatial competition and repulsion: pattern formation and the role of movement

Cristóbal López, Eduardo H. Colombo, Emilio Hernández-García and Ricardo Martínez-García

**Abstract** This chapter investigates some mechanisms behind pattern formation driven by competitive-only or repelling interactions, and explores how these patterns are influenced by different types of particle movement. Despite competition and repulsion are both anti-crowding interactions, collective effects may lead to clusters of individuals, which can arrange periodically. Through the analysis of two models, it provides insights into the similarities and differences in the patterns formed and underlines the role of movement in shaping the spatial distribution of biological populations.

## 1 Introduction

Collections of interacting particles are widely used to study complex systems, as they provide insights into diverse collective behaviors observed in various fields, such

---

Cristóbal López  
Instituto de Física Interdisciplinar y Sistemas Complejos (IFISC), CSIC-UIB, Campus Universitat Illes Balears, 07122 Palma de Mallorca, Spain e-mail: clopez@ifisc.uib-csic.es

Eduardo H. Colombo  
Center for Advanced Systems Understanding, (CASUS) – Helmholtz-Zentrum Dresden-Rossendorf (HZDR), Untermarkt 20, Görlitz, 02826, Germany

Emilio Hernández-García  
Instituto de Física Interdisciplinar y Sistemas Complejos (IFISC), CSIC-UIB, Campus Universitat Illes Balears, 07122 Palma de Mallorca, Spain

Ricardo Martínez-García  
Center for Advanced Systems Understanding, (CASUS) – Helmholtz-Zentrum Dresden-Rossendorf (HZDR), Untermarkt 20, Görlitz, 02826, Germany  
ICTP South American Institute for Fundamental Research & Instituto de Física Teórica, Universidade Estadual Paulista - UNESP, R. Dr. Bento Teobaldo Ferraz, 271 - 2 - Várzea da Barra Funda, São Paulo - SP, 01140-070, Brazil

as the flocking of animals [1], spatial patterns in ecosystems, embryos and colloids [2, 3, 4, 5], cell migration [6], and phase transitions in active matter [7]. Interactions among particles in these models occur via forces and/or dynamical rules which can be of physical, biological, or social origins, and can operate either locally, involving a few individuals, or over a finite distance, influencing many individuals and leading to long-range aggregates [8, 9].

The formation of these particle aggregates or clusters, that may appear forming global periodically ordered patterns, is particularly significant for biological populations like vegetation systems and cell populations [8, 9]. The spatial self-organisation has important ecological implications, producing feedbacks with biological functionalities that are fundamental for the biodiversity maintenance, population survival and the interactions with environmental factors [10]. A complete knowledge of the conditions that lead to these spatial structures and their feedback on the system dynamics is thus essential for the understanding of complex living systems.

In recent years, the authors have explored different models of pattern formation driven only by anti-crowding interactions through repelling forces and intraspecific competition (throughout this chapter we will refer to the both types of interactions as competing), and examined how these patterns are affected by particles' movement. Traditionally patterns in natural systems have been interpreted in terms of variations of the Turing mechanism [11], involving a combination of short-range attraction (facilitation) to start aggregation, and long-range repulsion (competition) to limit it spatially [8]. However, the pioneer works by Likoš and colleagues demonstrated that repulsive-only interactions in colloidal solutions and polymers could form cluster crystals, where clusters of particles organize into a crystalline structure [2, 12]. In biological contexts, it has been shown that competitive-only mechanisms (spatially non-local) can give rise to vegetation pattern formation [13], and species clustering in ecological niche space can occur despite competitive exclusion [14, 15].

This chapter presents results and discussions on two phenomena: pattern formation through anti-crowding interactions (which prevent individuals from getting too close to each other), and the role of movement on the spatial structure. Two different models of motile interacting individuals are discussed: one where particles repel each other via forces deriving from a soft potential, and another based on a birth-death model with competition rules. These models are studied using two complementary approaches: i) describing the particle dynamics, mainly based on off-lattice numerical simulations, and ii) a continuum mathematical description using partial differential equations for the number density of particles. Despite their differences, both models form the same type of patterns (cluster crystals) and, most importantly, under similar properties for the interaction. However, the underlying physical and/or biological mechanisms are completely different. The chapter also examines the influence of the type of movement of the organisms on the spatial structures. It has been noted that movement patterns of some living organisms are consistent with Lévy flight behavior [16, 17, 18], which has been argued to be advantageous over standard Brownian motion in certain foraging strategies [19]. This advantage primarily stems from the occurrence of occasional long jumps. These findings (and many others) highlight the importance of the type of movement when studying the spatial self-

organization of biological populations. However, the impact of Lévy-type diffusion on the properties of organism aggregates has not been extensively studied. Moreover, the importance of self-propelled motion (by which particles move consuming internal energy) is key to understand living systems [20]. We will briefly present some results concerning cluster formation with active (repelling) and Lévy particles.

The structure of this chapter is as follows. In Section 2 we present a comparative study of the pattern formation dynamics in the two discrete particle models. In Section 3 we analyze the impact of the type of motion on the spatial structures. Finally, Section 4 provides a summary and discussion.

## 2 Mechanisms of pattern formation for repelling/competing individuals

Here we present a comparative study of the pattern formation dynamics in two types of interacting particle systems. The first system consists of Brownian particles interacting via a repulsive soft potential [21]. The second one is a set of Brownian moving particles, with no forces among them but with a birth-death dynamics [22, 23]. For both models, we provide their mean-field density equation description to highlight the similarities in the interaction and diffusion conditions required to obtain spatial periodic patterns, and discuss the different physical mechanisms leading to these patterns.

### 2.1 A system of moving individuals with repulsive forces

Let us consider a system of  $N$  Brownian particles in contact with a thermal bath, in the overdamped limit, contained in a periodic two-dimensional domain. They interact through a soft-core (i.e. a potential not divergent at  $\mathbf{x} = 0$ ) repulsive two-body potential. The motion of the particles is given by

$$\dot{\mathbf{x}}_i = - \sum_{j=1}^N \nabla V(\mathbf{x}_i - \mathbf{x}_j) + \sqrt{2D} \boldsymbol{\xi}_i(t), \quad (1)$$

where the diffusion coefficient is  $D = k_B T / \gamma$ , with  $\gamma$  the friction coefficient,  $T$  the temperature of the bath, and Gaussian noise vectors  $\boldsymbol{\xi}_i$  satisfying

$$\langle \boldsymbol{\xi}_i \rangle = 0, \quad \langle \boldsymbol{\xi}_i(t) \boldsymbol{\xi}_j(t') \rangle = \mathbb{I} \delta_{ij} \delta(t - t'). \quad (2)$$

For the interaction potential we consider the generalized exponential model of exponent  $\alpha$  (GEM- $\alpha$ ), parameterized with exponent  $\alpha$ , widely used in many applications [12, 15]:

$$V(\mathbf{x}) = \epsilon \exp\left(-\left|\frac{\mathbf{x}}{R}\right|^\alpha\right). \quad (3)$$

$\epsilon$  is an energy scale and  $R$  a characteristic interaction range. Numerical simulations (see Fig. 1) confirm that hexagonal patterns spontaneously appear if  $\alpha > 2$  and the diffusivity is small enough. Patterns do not occur if  $\alpha \leq 2$ , independently of the value of the diffusion coefficient. For any  $\alpha$ , large values of the diffusivities give rise to a homogenous spatial distribution of particles.

This can be analytically understood by considering the Dean-Kawasaki (DK) equation [24] describing the system dynamics for the microscopic density of particles  $\rho(\mathbf{x}, t) = \sum_{i=1}^N \delta(\mathbf{x} - \mathbf{x}_i(t))$ . In fact, to reproduce the phenomenology presented here it is enough to consider its deterministic version, i.e. the one obtained by neglecting stochastic noise terms, which is appropriate for sufficiently large density of particles, and amounts to a kind of mean-field description:

$$\partial_t \rho(\mathbf{x}, t) = \nabla \cdot \left( \rho(\mathbf{x}, t) \int d\mathbf{x}' \nabla V(\mathbf{x} - \mathbf{x}') \rho(\mathbf{x}', t) \right) + D \nabla^2 \rho(\mathbf{x}, t). \quad (4)$$

The diffusion term results from the random motion of Brownian particles, while the potential term describes density advection by the local velocity due to repulsive forces. Note the conservative character of this equation (it is of continuity type) reflecting that the total number of particles in the system remains constant. Numerical simulations confirm that it properly describes the density of the particle system at large scales [21], in regimes where fluctuations can be neglected. Any constant density  $\rho_0$  is a solution of Eq. (4). We perform a linear stability analysis around this homogeneous solution by considering a small perturbation  $\rho(x, t) = \rho_0 + \exp(\lambda t + i\mathbf{k} \cdot \mathbf{r})$ , which gives the following dispersion relation, or growth rate:

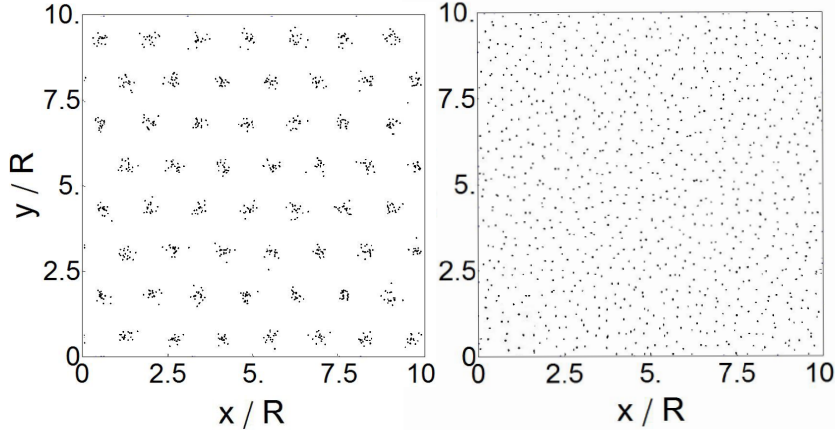


**Fig. 1** Snapshot of the positions of  $N = 1000$  particles at large times, moving according to Eq. (1), for  $R = 0.1$ ,  $\epsilon = 0.033$ , and  $L = 1$ . Left plot is for the GEM-3 potential, i.e.  $\alpha = 3$  and  $D = 0.02$ . The right plot is for GEM-1 ( $\alpha = 1$ ) and  $D = 0.005$ . Modified from [21].

$$\lambda(k) = -k^2 [D + \rho_0 \hat{V}(k)], \quad (5)$$

with  $\hat{V}(k)$  the Fourier transform of the interaction potential ( $k = |\mathbf{k}|$ ). A positive value of  $\lambda(k)$  for some  $k$  reveals a pattern-forming instability in which perturbations of periodicity  $2\pi/k$  will grow on top of the homogeneous density  $\rho_0$ , leading to pattern formation with that periodicity. Note that a necessary condition for  $\lambda(k) > 0$  is that the Fourier transform of the potential takes negative values for some values of  $k$  [23]. This explains why patterns can never be observed with, for example, GEM-1 or GEM-2 potentials, whose Fourier transforms are always positive. In general, the Fourier transform of the GEM- $\alpha$  potential is always positive if  $\alpha \leq 2$ . This is consistent with numerical simulations of the density equation, Eq. (4), which lead to a homogeneous state for  $\alpha \leq 2$  [21], and analogously for the particle system. For  $\alpha > 2$ , however, the potential is more box-shaped, leading to Fourier transforms that may have negative values [15]. Note that for the derivation of Eq. (5) to hold, the soft character of the potential is crucial since otherwise, i.e., the hard-core case, its Fourier transform is not properly defined and another methodology is needed [25]. Also, in Eq. (5) we observe that the growth rate  $\lambda(k)$  is always negative for large values of  $D$ , so that large diffusion coefficient inhibits pattern formation and makes the spatial distribution of particles homogeneous.

Eq. (5) shows the mathematical conditions for the instability of the homogenous solution in the continuum density description of the system of particles. A detailed study performed in [21] indicates that physically the formation of clusters comes from a balance between the internal repulsion of particles inside a cluster, and the external repulsion from the particles in neighboring clusters (see Fig. 2), and mediated by the diffusion of the particles. Thus, when diffusion is small and repulsion from particles in neighboring clusters dominates the internal repulsion with other particles in the same cluster, aggregation tends to be enhanced.

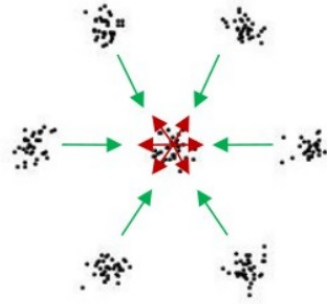


**Fig. 2** Schematic representation of balance of forces between neighboring clusters (green) and neighboring particles inside a cluster (red).

## 2.2 A system of birth-death particles

Let us consider a system of initially  $N_0$  particles performing random Brownian motion with diffusivity  $D$  in a two-dimensional square with periodic boundary conditions. In addition, the particles undergo a birth-death dynamics, so that the total number of them is not constant, and there are  $N(t)$  particles in the system at time  $t$ . The demographic events occur at stochastic Poisson times with the following rates per particle: i) at rate  $\beta_0$  one particle is chosen to die, i.e. to disappear from the system; ii) particle  $i$  is chosen with rate  $\lambda_i$  to reproduce, with the offspring being placed at the same location as the parent. The important point is that the birth rate  $\lambda_i$  diminishes with the number of particles within a radius  $R$  from the focal particle  $i$ . This is a kind of competing dynamics since the birth rate of a given individual decreases with the number of others in its surroundings, which maybe due to competition for resources or mates. More explicitly, the rate  $\lambda_i$  at which a new particle is introduced in the system, exactly at the location of the parent particle  $i$ , is  $\lambda_i = \lambda_0 - g N_R^i$ , where  $\lambda_0$  and  $g$  are constants, and  $N_R^i$  is the number of particles around  $i$  within a radius  $R$ .

We can consider more generally that this neighborhood dependence is weighted with the distance. The weight is expressed through an *influence* function that decays with the distance between the particles and the focal one  $G(\mathbf{x}_i - \mathbf{x}_j)$ ,  $j = 1, \dots, N(t)$ . In this way, particle  $i$  will give rise to the birth of a new particle at its position with a probability rate  $\lambda_i = \lambda_0 - g \sum_{j \neq i} G(\mathbf{x}_i - \mathbf{x}_j)$ . The previous case is recovered for a top-hat function  $G(\mathbf{x})$ , i.e. a constant if  $|\mathbf{x}| < R$  and 0 otherwise.

Two transitions can be identified in the system:

1. An absorbing transition that differentiates between the absorbing phase, where all particles are dead (i.e. there are no particles in the system), and an active phase. In the active phase, at large times and high values of  $\mu = \lambda_0 - \beta_0$  (the parameter driving the transition), the system contains many particles.
2. Depending on the shape of the influence function,  $G$ , and if the diffusion coefficient of the particles is sufficiently small, the particles may arrange into a hexagonal pattern, as illustrated in Fig. 3 for a top-hat influence function. The plot also shows the statistically homogeneous distribution that occurs when the diffusion coefficient is large.

Note that the pattern structure resembles that observed in the system of repulsive particles (Fig. 1). However there are significant differences between the two models. The system of repelling particles is in equilibrium with a thermal bath and the total number of particles is conserved. In contrast, the birth-death system is a prototypical non-equilibrium system, characterized by the presence of an absorbing configuration, and the number of particles fluctuates and is not conserved (although its average reaches a constant value at long times).

We can further explore the analogies and differences by examining the deterministic macroscopic density equation for this system with an arbitrary influence function  $G$ . This equation was derived using field theoretical techniques in [22]. As before, we neglect here the stochastic terms so that a mean-field version of it is given

by

$$\partial_t \rho(\mathbf{x}, t) = \rho(\mathbf{x}, t) \left( \mu - g \int d\mathbf{x}' G(\mathbf{x} - \mathbf{x}') \rho(\mathbf{x}', t) \right) + D \nabla^2 \rho(\mathbf{x}, t). \quad (6)$$

Here, the influence function is usually normalized so that  $\int G(\mathbf{x}) d\mathbf{x} = 1$ . Note that Eq. (6) is not a continuity equation as Eq. (4), indicating that the total number of particles is not conserved now. A linear stability analysis of Eq. (6) is also straightforward. Again considering a perturbation around the homogenous solution,  $\rho_0 = \mu/g$ , we obtain the following growth rate

$$\lambda(k) = -(Dk^2 + \mu \hat{G}(k)), \quad (7)$$

where  $\hat{G}(k)$  is the Fourier transform of the influence function. Note the similarity between this expression and Eq. (5). A necessary condition for pattern formation is that the Fourier transform of the influence function has negative values, which is the same condition required for the potential in the system of repelling particles (numerical simulations of the density equation, Eq. (6), confirm this scenario [22]). But the underlying mechanism is quite different. Patterns appear due to the presence of exclusion zones, which are spatial zones between the clusters (at distances larger than  $R$  and smaller than  $2R$ ) that fall within the range of influence of two clusters. In these zones, particles face enhanced competition as they must compete with particles from both clusters. This phenomenon is similar to that observed in some nonlocal vegetation models, where exclusion areas were first identified [13]. See Fig. 4 for a visual explanation of this concept. Note that, when spacing is fixed by the interaction range, hexagonal patterns naturally result from self-organization due to competitive

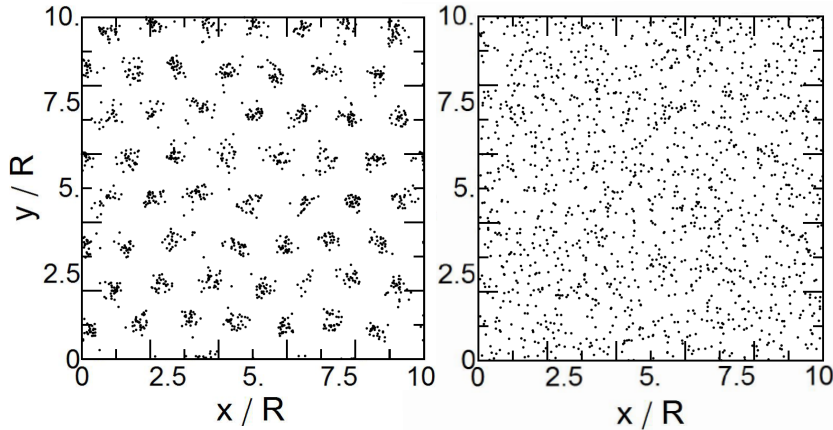


**Fig. 3** Long-time spatial structures for the birth-death model with the top-hat influence function, i.e. birth rate  $\lambda_i = \lambda_0 - gN_R^i$ , where  $N_R^i$  is the number of neighbors within distance  $R$  from particle  $i$ .  $R = 0.1$ , system size  $L = 1$ ,  $g = 0.02$ . Left:  $D = 10^{-5}$ ,  $\lambda_0 = 0.85$  and  $\beta_0 = 0.15$ , so that  $\mu = \lambda_0 - \beta_0 = 0.7$ . Right:  $D = 10^{-4}$ ,  $\lambda_0 = 0.95$  and  $\beta_0 = 0.05$ , so that  $\mu = 0.9$ . The largest diffusion coefficient destroys the spatial pattern. Modified from [22].

interactions. This configuration maximizes the exclusion area while maintaining spacing. However, more complex models can produce other structures like stripes [26].

### 2.3 Discussion on the influence function

The models discussed in the previous section are phenomenological effective descriptions of populations of interacting individuals. Real interactions, specially in biological contexts, are often mediated by agents, visual or chemical signals, or substances (in general called mediators) whose temporal dynamics is usually faster than that of the population. A more fundamental description of the system should explicitly consider these signal dynamics, with the effective mathematical equations (e.g. Eq. (6)) derived through the adiabatical elimination of the signal dynamics. However, there is no systematic derivation of the population dynamics leading to arbitrary influence functions keeping the character of competitive-only interactions. In cases where such a derivation has been provided, the resulting equations did not have the characteristics necessary for pattern formation [26] (in vegetation systems), or, although leading to patterns, the influence functions lack of generality [27] (in the context of cell dynamics).

A new mechanism has been proposed that allows for the derivation of more general influence functions, including those with a shape similar to the GEM- $\alpha$  function [28, 29], in particular with cases leading to non-positive Fourier transforms. Briefly, this mechanism considers that mediators are released into the environment in the form of short pulses. The response to these pulse releases can significantly change the spatial stability of the population. In particular, in the limit of fast mediator dynamics, an effective description for the single population emerges, where the influence function is general enough and capable of leading to spatial instabilities.

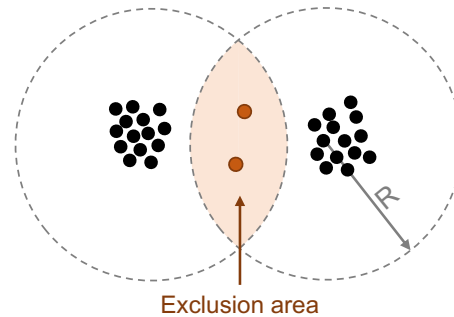


**Fig. 4** Schematic representation of the formation of exclusion areas (orange shaded region), where individuals have to compete with two different clusters, whereas individuals in each patch compete only with individuals in its own patch.

### 3 Role of motion on spatial structure

In the models of the previous Section, despite their profound differences, we observed that the same ingredients are key for pattern formation: the spatial shape of the function (the potential or the influence) giving the particle interactions and a low enough diffusivity. Having focused on the role of interactions in the earlier sections, we will now discuss deeper the role of motility, considering two types: Lévy flights and active motion. First, we will analyse the impact of Lévy on the birth-death model, and then we will briefly examine the effects of active motion on the system of repulsive particles. Given the numerous analogies in the descriptions of both models, many of the results discussed for one system are applicable to the other.

As demonstrated both using the discrete particle dynamics and the instability analysis of the continuum description, clusters disappear and the population shows a uniform distribution for Brownian particles moving *very randomly*, i.e., when their diffusion coefficient is large. A natural question arises: what happens in the system if particles exhibit other types of motion? Of particular biological relevance is to consider particles performing Lévy flights or active motion.

Lévy flights results in movement patterns that are statistically different to Brownian motion. The displacement lengths have a power-law distribution resulting in the alternation of frequent, short displacements, with rare, long ones. Due to the weight of these long jumps, the variance of the displacement length is infinite, which translates into an infinite diffusion coefficient. Yet, one can still define a generalized diffusion coefficient,  $\kappa_\gamma$ , such that the typical displacement of an individual particle scales as  $x \propto (\kappa_\gamma t)^{1/\gamma}$ , where  $0 < \gamma < 2$  is the Lévy index or anomalous exponent which determines the type of motion. The smaller the value of  $\gamma$  the more anomalous is the random walk (more frequent are long jumps). The question is whether the formally infinite diffusion coefficient destroys the spatial patterns. To analyze the impact of Lévy type of motion and spatial patterns we, as mentioned, will focus on the birth-death system (see [30]). We consider the same demographic processes as in Sec.2.2 but instead of Brownian motion the particles perform Lévy flights.

As shown in [30], see also Fig. 5, clusters are not broken by the infinite diffusion coefficient of Lévy flights. However, large jumps do influence the characteristics of the patterns: clusters are less compact, and many single particles are found moving between them. The large-scale properties of the system can be derived from the mean-field density equation, which now, in terms of the fractional Laplacian  $\nabla^\gamma$ , takes the form:

$$\partial_t \rho(\mathbf{x}, t) = \rho(\mathbf{x}, t) \left( \mu - g \int d\mathbf{x}' G(\mathbf{x} - \mathbf{x}') \rho(\mathbf{x}', t) \right) + \kappa_\gamma \nabla^\gamma \rho(\mathbf{x}, t). \quad (8)$$

Doing a stability analysis similar to the previous cases we obtain the following perturbation growth rate

$$\lambda(k) = -(\kappa_\gamma k^\gamma + \mu \hat{G}(k)), \quad (9)$$

where  $\hat{G}(k)$  is the Fourier transform of the influence function. There are no essential differences between Eq. (9) and Eq. (7). As shown in [30] the Lévy index  $\gamma$  has only a small impact on the properties of the pattern.

One can conclude that the large-scale collective behavior of the system is more strongly influenced by the competitive interactions than by the type of motion performed by the particles. The long flights characteristics of Lévy movement do not accumulate their effect enough to break clusters. However, this is of course not always the case, as demonstrated by the consideration of active motion. [31, 32] explored a simple extension of the system of repulsive particles Eq. (1) by introducing an internal degree of freedom: the orientation of a self-propulsion speed. This results in a system of active Brownian particles interacting in pairs through a repulsive potential. Briefly, activity has two main effects on the distribution of particles (when the diffusivity of the particles is small, and thus clusters form in the absence of activity): a) For high values of the self-propulsion velocity, clusters are destroyed, and the steady-state becomes statistically homogeneous (the cluster crystal melts). This effect is similar to an enhanced effective diffusivity of the particles. b) For intermediate values of the self-propulsion velocity, particle density within clusters is depleted, see Fig. 6, so that they reach a ring-like shape. This is a striking effect induced by the self-propelled motion.

## 4 Summary and conclusions

We have presented a comparative study of two types of motile competing particle systems. Despite their significant differences, both of them exhibit similar spatial patterns that are induced by the same conditions for the interactions and the diffusivity of the individuals. However, the underlying physical or biological mechanisms differ substantially. We also analyzed the role of motion on patterns characteristics. In

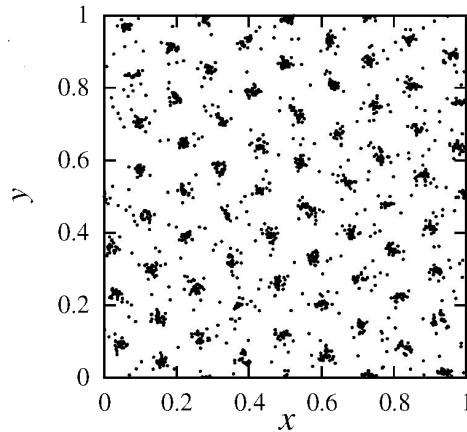


**Fig. 5** Particle configuration at long times for particles interacting as in Fig. 3, but with Lévy motion with Lévy index  $\gamma = 1$  and  $\kappa_\gamma = 56 \times 10^{-5}$ . Other parameters:  $R = 0.1$ ,  $L = 1$ ,  $\lambda_0 = 1$ ,  $\beta_0 = 0.1$ ,  $g = 0.02$ . Modified from [30].

the case of Lévy flights, we concluded that their impact is less significant than that of the interactions. Competitive interactions are the main drivers of the global spatial structure of the system. However, striking impacts were observed when we considered active motion, for example making single aggregates of particles become rings.

The examples we showed highlight an important observation in the literature on pattern formation studies: while analyzing the properties of structures can be challenging, it often does not reveal the underlying natural mechanisms or the functionalities of the individuals that are organized in such spatial distributions. However, numerous studies show that pattern formation is key to understand the factors leading to survival, the proper response to external factors, and ecological and evolutionary processes in biological dynamics. For instance, there is a known spatial pattern sequence to desertification in water-limited ecosystems, so that it may serve as early warning signal [33]. At much smaller scales, the spatial organization of cells is essential for accurately characterizing, forecasting and controlling tumor evolution [34]. For non-neutral species, patterns may enable weaker competitors to survive in conditions that would otherwise lead to their extinction when spatial distribution is ignored [35]. In the context of the birth-death model we presented, it has been shown that when two otherwise identical types of particles compete, the type dispersing less and forming more compact clusters, due to its type of motion, is more likely to survive [36].

Regarding the interplay between spatial dispersion of organisms and their mobility, it is worth mentioning an emerging field known as proliferating active matter, which considers demographic dynamics in addition to the other factors. This field combines elements of the two models presented in this chapter, along with self-propulsion, and offers a natural framework for studying many biological systems [37].

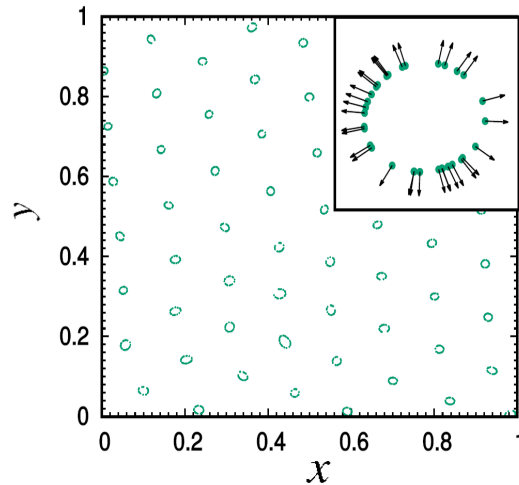


**Fig. 6** Ring-shaped clusters appearing in a system of self-propelled repulsive particles. The inset shows the orientation of the self-propulsion velocity of the particles in a given cluster. Taken from [32].

In conclusion, we believe that gaining a deeper understanding of the feedbacks between spatial structure, interactions and individual motility will provide valuable insights into the dynamics of living complex systems.

**Acknowledgements** C.L. acknowledges the warm hospitality at the Isaac Newton Institute for Mathematical Sciences (INI) during the program *Mathematics of movement: An interdisciplinary approach to mutual challenges in animal ecology and cell biology*. He also acknowledges the Scultetus Visiting Scientist Program at the Center for Advanced Systems Understanding (CASUS) in Görlitz, Germany, where this work was completed. C.L. and E.H-G. acknowledge grant LAMARCA PID2021-123352OB-C32 funded by MCIN/AEI/10.13039/501100011033323 and FEDER "Una manera de hacer Europa"; and Grant TED2021-131836B-I00 funded by MICIU/AEI/10.13039/501100011033 and by the European Union "NextGenerationEU/PRTR". E.H-G. also acknowledges the Maria de Maeztu program for Units of Excellence, CEX2021-001164-M funded by MCIN/AEI/10.13039/501100011033. E.H.C. and R.M-G. are partially funded by the Center of Advanced Systems Understanding (CASUS), which is financed by Germany's Federal Ministry of Education and Research (BMBF) and by the Saxon Ministry for Science, Culture and Tourism (SMWK) with tax funds on the basis of the budget approved by the Saxon State Parliament.

## References

1. Cavagna, A., Giardina, I., *Annual Review of Condensed Matter Physics* **5**, 183 (2014).
2. Likos, C.N., Mladek, B.M., Gottwald, D., Kahl, G., *The Journal of Chemical Physics* **126** (2007).
3. Rietkerk, M., van de Koppel, J., *Trends in Ecology and Evolution* **23** (3), 169 (2008).
4. Baker, R.E., Gaffney, E.A., Maini, P.K., *Nonlinearity* **21**, R251 (2008).
5. Borgogno, F., D'Odorico, P., Laio, F., and Ridolfi, L., *Reviews of Geophysics* **47** (2009).
6. Alert, R., Trepast, X., *Annual Review of Condensed Matter Physics* **11**, 77 (2020).
7. Cates, M.E., Tailleur, J., *Annual Review of Condensed Matter Physics* **6**, 219 (2015).
8. Murray, J.D.: *Mathematical Biology: II: Spatial Models and Biomedical Applications* vol. 18. Springer, New York (2003).
9. Martínez-García, R., Tarnita, C.E., Bonachela, J.A., *Emerging Topics in Life Sciences* **6** (3), 245 (2022).
10. Wiegand, T., et al., *Nature Ecology & Evolution* volume **5**, 965 (2021).
11. Turing, A., *Philosophical Transactions of the Royal Society of London B* **237** (641), 37 (1952).
12. Mladek, B.M., Gottwald, D., Kahl, G., Neumann, M., Likos, C.N., *Physical Review Letters* **96**, 045701 (2006).
13. Martínez-García, R., Calabrese, J.M., Hernández-García, E., López, C., *Geophysical Research Letters* **40**, 6143 (2013).
14. Scheffer, M., Van Nes, E.H., *Proc. Natl. Acad. Sci. USA* **103**, 6230 (2006).
15. Pigolotti, S., López, C., Hernández-García, E., *Physical Review Letters* **98**, 258101 (2007).
16. Metzler, R., Klafter, J., *Physics Reports* **339**, 1 (2000).
17. Dieterich, P., Klages, R., Preuss, R., Schwab, A., *Proc. Natl. Acad. Sci. USA* **105**, 459 (2008).
18. Viswanathan, G. M., Raposo, E. P., da Luz, M. G. E., *Physics Life Reviews* **5**, 133 (2008).
19. Bartumeus, F., Peters, F., Pueyo, S., Marrasé, C., Catalán, J., *Proc. Natl. Acad. Sci. USA* **100**, 12771 (2003).
20. Marchetti, M. C., Joanny, J. F., Ramaswamy, S., Liverpool, T. B., Prost, J., Madan Rao, and Aditi Simha, R., *Rev. Mod. Phys.* **85**, 1143 (2013).
21. Delfau, J.B., Ollivier, H., López, C., Blasius, B., Hernández-García, E., *Physical Review E* **94** (4), 042120 (2016).
22. Hernández-García, E., López, C., *Physical Review E* **70**, 016216 (2004).
23. López, C., Hernández-García, E., *Physica D: Nonlinear Phenomena* **199** (1), 223 (2004).
24. Dean, D.S., *Journal of Physics A: Mathematical and General* **29**, L613 (1996).
25. Caprini, L., Hernández-García, E., López, C., *Physical Review E* **98** (5), 052607 (2018).
26. Martínez-García, R., Calabrese, J.M., Hernández-García, E., López, C., *Philosophical Transactions of the Royal Society of London A: Mathematical, Physical and Engineering Sciences*, **372**, 20140068 (2014).
27. Mogilner, A.: *Modelling spatio-angular patterns in cell biology*. PhD thesis, University of British Columbia (1995).
28. Colombo, E. H., López, C., Hernández-García, E., *Phys. Rev. Lett.* **130**, 058401 (2023).
29. Colombo, E. H., Martínez-García, R., Calabrese, J.M., López, C., Hernández-García, E., *J. Stat. Mech.* **2024** 034001 (2024).
30. Heinsalu, E., Hernández-García, E., López, C., *Europhysics Letters* **92** (4), 40011 (2010).
31. Delfau, J.B., López, C., Hernández-García, E., *New Journal of Physics* **19**, 095001 (2017).
32. Caprini, L., Hernández-García, E., López, C., Marini Bettolo Marconi, U., *Scientific Reports* **9** (1), 16687 (2019).
33. Kéfi, S., Rietkerk, M., Alados, C. et al. *Nature* **449**, 213 (2007).
34. Bellomo, N., Li, N.K., Maini, P.K., *Mathematical Models and Methods in Applied Sciences* **18**, 593 (2008).
35. Maciel, G.A., Martínez-García, R., *Journal of Theoretical Biology* **530**, 110872 (2021).
36. Heinsalu, E., Hernández-García, E., López, C., *Phys. Rev. Lett.* **110**, 258101 (2013).
37. Hallatschek, O., Datta, S.S., Drescher, K., Dunkel, J., Elgeti, J., Waclaw, B., and Wingreen, N.S., *Nature Reviews Physics* **5**, 407 (2023).